PNAS
www.pnas.org

Supplementary Information for

Oncostatin M-induced astrocytic tissue inhibitor of metalloproteinases-1 drives remyelination

Evelien Houben[1,*], Kris Janssens[1,*], Doryssa Hermans[1], Jennifer Vandooren[2], Chris Van den Haute[3,4], Melissa Schepers[1,5], Tim Vanmierlo[1,5], Ivo Lambrichts[6], Jack van Horssen[1,7], Veerle Baekelandt[3], Ghislain Opdenakker[2], Wia Baron[8], Bieke Broux[1,*], Helena Slaets[1,*], Niels Hellings[1,*]

[1]Department of Immunology, Biomedical Research Institute, Hasselt University, 3590 Diepenbeek, Belgium
[2]Department of Microbiology and Immunology, Laboratory of Immunobiology, Rega Institute, KU Leuven, 3000 Leuven, Belgium
[3]Department of Neurosciences, Laboratory for Neurobiology and Gene Therapy, KU Leuven, 3000 Leuven, Belgium
[4]Leuven Viral Vector Core, KU Leuven, 3000 Leuven, Belgium
[5]School for mental health and neuroscience, division translational neuroscience Maastricht University, 6200MD, Maastricht, The Netherlands
[6]Department of Morphology, Biomedical Research Institute, Hasselt University, 3590 Diepenbeek, Belgium
[7]Department of Molecular Cell Biology and Immunology, Amsterdam Neuroscience, Amsterdam University Medical Center, location VU University medical center, MS Centrum, 1007 MB Amsterdam, Netherlands
[8]Section Molecular Neurobiology, Department Biomedical Sciences of Cells & Systems, University of Groningen, University Medical Center Groningen, 9713 AV Groningen, the Netherlands
[*] *These authors contributed equally to this work*

Niels Hellings
Email: niels.hellings@uhasselt.be

This PDF file includes:

www.pnas.org/cgi/doi/10.1073/pnas.1912910117

Materials and methods

Animals

OSMRβ knock-out (KO) mice were provided by the RIKEN BRC through the National Bio-Resource Project of MEXT, Japan, and were generated as previously described (1, 2). B6.129S4-Timp1^{tm1Pds}/J KO mice were purchased from Jackson Laboratories (Main, USA). All mice had a C57BL/6JOlaHsd background and wild type (WT) mice were back-crossed with the genetically modified animals to obtain a genetically identical background. For experiments with CNS-targeted lentiviral (LV) overexpression, seven week old male C57BL/6J mice were purchased from Envigo (Horst, the Netherlands). Wistar rats were purchased from Charles River (Chatillon-sur-Chalaronne, France). Animals were housed in an accredited conventional animal facility under a 12h light/dark cycle and had free access to food and water. All animal procedures were in accordance with the EU directive 2010/63/EU and all mouse experiments were approved by the Hasselt University Ethics Committee for Animal Experiments. All rat experiments were approved by the Institutional Animal Care and Use Committee of the University of Groningen.

Cuprizone treatment

Eight week old mice were fed a diet containing 0.2% cuprizone (Sigma-Aldrich, Bornem, Belgium), which was homogenously mixed into powdered rodent chow and renewed three times a week. Two experimental set-ups were applied. First, OSMRβ KO or TIMP-1 KO and WT mice received a 0.2% cuprizone diet for five weeks to induce acute demyelination, followed by one or two weeks of standard diet to allow spontaneous remyelination. Second, to reveal the effect of CNS-targeted LV-OSM treatment on remyelination, mice were fed with a 0.2% cuprizone diet for 12 weeks to induce chronic demyelination, followed by one or two weeks of standard diet to allow remyelination. Chronic demyelination largely hampers subsequent spontaneous remyelination, as observed in chronic MS lesions (3). After 11 weeks of cuprizone diet, mice were stereotactically injected with LV-OSM or LV-enhanced green fluorescent protein (eGFP) (details see below).

Lentiviral vector construction and administration

The murine OSM gene transcript (NM_001013365) was isolated from RAW 264.7 cells (ATCC, Molsheim, France) after stimulation with 100 ng/ml LPS (Sigma-Aldrich) for 24h. Complementary DNA was cloned into a lentiviral (LV) transfer plasmid containing a central polypurine tract sequence, the SIN-18 deletion and the woodchuck hepatitis posttranscriptional regulatory element (4). HIV-1-derived vector particles were produced by a triple transient transfection of 293T cells, as previously described (5). Briefly, cells were transfected with a second-generation packaging plasmid, a plasmid encoding the glycoprotein G of vesicular stomatitis virus and a transfer plasmid encoding the OSM cDNA under control of a cytomegalovirus promoter. This mixture, combined with a 1.42 µM polyethyleneimine solution in 150 mM NaCl, was added to 293T cells in OPTI-MEM (Life technologies, Gent, Belgium) free of serum. Vector particles in the supernatant were collected and filtered 48h and 72h post transfection and concentrated using Vivaspin 15 columns (Vivascience, Hannover, Germany). p24 antigen content was measured using HIV-1 p24 Core Profile ELISA (DuPont, Dreieich, Germany). After 11 weeks of 0.2% cuprizone diet, mice were stereotactically injected with 4 µl of LV-OSM or LV-eGFP ($3.43*10^7$ pg of p24/ml) in the right striatum with a speed of 0.25 µl/minute, as previously described (6, 7). Coordinates for injection were anteroposterior 0.5 mm, lateral 2.2 mm and dorsolateral -2.5 mm (2µl) and -2.0 mm (2µl) using Bregma as reference.

Tissue collection

Brains of healthy and cuprizone-treated mice (n=4, 5 or 6 per group) were isolated and snap-frozen in liquid nitrogen after transcardial perfusion with Ringer's solution. For the OSMRβ KO and LV-OSM treatment experiments, tissue preparation was performed from whole brain. After stereotactical injection in the LV-OSM treatment experiments, the whole brain was sectioned in a left part (contralateral), a middle part (containing the CC) and a right part (transduced). mRNA levels were assessed with qPCR after one week of remyelination and protein levels after two weeks of remyelination via immunohistochemical analysis. For the TIMP-1 KO experiments, tissue for all *ex vivo* analyses was derived from the same animals. The posterior part (around bregma -1.82 mm) of the brain was used for immunohistochemistry, the corpus callosum (CC) (1 mm thick) within

the anterioposterior coordinates from -0.82 to -1.82 mm was used for mRNA isolation. Analysis of mRNA levels was performed with the use of qPCR after two weeks of remyelination. Protein levels were determined after two weeks of remyelination by immunohistochemical analysis.

Primary astrocytes

Brains were dissected from P2 C57BL/6J mouse pups and the meninges were removed to obtain the cortices. The cortices were then resuspended by incubation in papain solution at 37°C for 20min. The cell suspension was washed and triturated using sterile glass Pasteur pipettes. The mixed glial culture was transferred to a poly-L-lysine (5 µg/ml) coated flask containing DMEM (Life technologies) supplemented with 10% fetal calf serum (Hyclone Europe, Erembodegem, Belgium), 50 U/ml penicillin and 50 mg/ml streptomycin (Life technologies) and incubated at 37°C and 8.5% CO_2. After 14 and 21 days non-adherent cells (oligodendrocytes and microglia) were removed by shaking the flask at 220 rpm overnight at 37°C to obtain primary astrocytes. The purity of the astrocyte cultures was assessed with flow cytometry using chicken anti-GFAP PE (Novus Biologicals, Abingdon, England). All cell cultures had a purity above 95%. To obtain astrocyte conditioned medium (ACM) $4x10^6$ astrocytes were seeded in T75 flasks and treated with or without 25 ng/ml recombinant mouse OSM protein (rmOSM) in DMEM (12 ml) for three constitutive days. For the OPC differentiation experiments (see below), the medium was replaced after these three days by SATO medium (12 ml) for 24h.

Primary oligodendrocyte precursor cells

Primary rat OPCs were isolated as previously described (8). In short, OPCs were derived from the neonatal cortex of P1-2 Wister rats (Charles River), using a shake-off procedure (8). Two days before treatment, the OPCs were treated with 10 ng/ml platelet-derived growth factor-AA (PDGF-AA, Peprotech, cat. no. 100-13A) and 10 ng/ml human fibroblast growth factor-2 (FGF-2, Peprotech, cat. no. 100-18B) to synchronize these to the bipolar early OPC stage. Thereafter, OPCs were treated with 10 ng/ml recombinant rat TIMP-1 (rTIMP-1) (R&D Systems) for three (immature oligodendrocytes) or six days (mature oligodendrocytes) to allow differentiation. For the ACM experiment, OPCs were treated with ACM (dilution 1:10) from WT and TIMP-1 KO astrocytes

treated with or without OSM (25 ng/ml) for three days. TIMP-1 concentrations in these ACM dilutions were determined by ELISA (see below): WT-OSM ACM: 9.6±0.3 ng/ml TIMP-1; WT-no OSM: 1.8±1.3 ng/ml TIMP-1; KO-OSM: not detected; KO-no OSM: not detected.

Enzyme-linked immunosorbent assay (ELISA)

TIMP-1 concentrations were quantified using the mouse TIMP-1 (DY980) DuoSet ELISA kit (R&D Systems) and the DuoSet Ancillary Reagent Kit 2 (DY008; R&D Systems), according to the manufacturer's instructions.

Histochemistry

Ten micrometer cryosections were cut using the Leica CM3050S cryostat (Leica Microsystems, Wetzelar, Germany). Luxol Fast Blue (LFB) staining was performed by fixing the cryosections in acetone, followed by incubation in LFB solution at 56°C for 16h. Sections were then differentiated in 0.5% lithium carbonate solution and counterstained with cresyl violet (Sigma-Aldrich). Image collection was performed using Leica DM2000 LED and Leica Application Suite software (Leica Microsystems, Diegem, Belgium). The amount of myelinated area in the CC was quantified using ImageJ software (n=4 or 5 animals per group; 3 sections per animal). The threshold was set so that the non-myelinated regions (cortex) were below threshold.

For immunohistochemistry, sections were fixed in acetone, blocked with 10% goat serum and incubated with rabbit anti-NG2 (1:200, Millipore, Overijse, Belgium), mouse anti-GFAP (1:500, Sigma-Aldrich), rat anti-TIMP-1 (1:50, Abcam, Cambridge, UK) and goat anti-OSM antibodies (1:50, R&D Systems, Abingdon, UK). Binding of the primary antibodies was visualized with Alexa 488- or Alexa 555-conjugated secondary antibodies (Life technologies) and nuclear staining was performed with 4',6-diamidino-2-phenylindole (DAPI, Life technologies). Oligodendrocyte lineage of NG2+ cells was confirmed with OLIG2 (1:50, Bio-Techne, Abingdon, UK) double staining. The number of $NG2^+$ cells and the $GFAP^+$ areas were measured in 4 to 5 animals per group (6 photos per animal) using the Nis-Elements software. For mouse anti-CC-1 immunostaining (1:200, Millipore) the Vector® Mouse On Mouse Immunodetection Kit (Vector Laboratories, Peterborough, UK) was used according to the manufacturer's instructions. The number of $CC1^+$ cells in the CC

was counted in 4 to 5 animals per group (6 photos per animal) based on the presence of nuclei using the Nis-Elements software. All analyses of de- and remyelination on mice tissue were performed in the CC, since this area represents the most frequently investigated white matter tract in the cuprizone model (9, 10).

Human brain tissue samples (n=4; containing 3 active and 3 chronic active white matter lesions) were obtained from the Netherlands Brain Bank (NBB, Amsterdam, the Netherlands). Formalin-fixed paraffin embedded tissue sections of 10 µm were deparaffinized in xylene and rehydrated through a graded alcohol series into distilled water. Next, 0.3% hydrogen peroxidase diluted in methanol was used to quench endogenous peroxidase activity. For HLA-DR and TIMP-1 heat-induced antigen retrieval was performed using 10 mM sodium citrate buffer (pH 6.0). Sections for the PLP staining were blocked with 100% protein block (DAKO) and for the HLA-DR staining 10% protein block (DAKO) in PBS was used. Blocking for TIMP-1 was performed for 20min with 1% protein block (DAKO)/0.05% Tween20 in BPS. Sections were rinsed in PBS and incubated overnight with mouse-anti-PLP (1:100, BIO-RAD, Temse, Belgium), mouse-anti-HLA-DR (1:50, clone LN3, Thermo Fisher Scientific) both diluted in 10% protein block (DAKO) in PBS or mouse-anti-TIMP-1 (1:100, Thermo Fisher Scientific), goat-anti GFAP (1:400, Santa Cruz, Huizen, the Netherlands) both diluted in 10% protein block (DAKO) and 0.05% Tween20 in PBS at 4°C. The next day, tissue sections were rinsed in PBS and incubated with DAKO EnVision^{+} Dual Link System-HRP (Dako, Carpinteria, USA) for 30min at room temperature. Diaminobenzidine tetrachloride (DAB) chromogen system (Dako) was used for visualization. After washing with distilled water, sections were incubated with hematoxylin for 2min and extensively rinsed with tap water. Finally, the tissue sections were dehydrated with an ethanol series followed by xylene. For the TIMP-1/GFAP fluorescent double staining the primary antibodies were visualized with Alexa 488- or Alexa 555-conjugated secondary antibodies (Life technologies) and the nuclear staining was performed with 4',6-diamidino-2-phenylindole (DAPI, Life technologies). Image collection was performed using Leica DM2000 LED and Leica Application Suite software (Leica Microsystems). All analyses were conducted in a blinded manner.

Immunocytochemisty

Cells were fixed with 4% paraformaldehyde for 20min at room temperature. OPCs were permeabilised with 0.1% Triton X-100 in 4% BSA and astrocytes with 0.2% Triton X-100 in 3% goat serum for 30min, followed by 60min incubation with rat anti-MBP antibodies (1:250, Serotec) or 2.5h incubation with rat anti-TIMP-1 (1:100, Abcam). Next, cells were washed with PBS, and incubated for 25min (OPCs) or 1h (astrocytes) with the appropriate TRITC-conjugated secondary antibody (1:50, Jackson Immunoresearch or 1:350, Lifetechnologies). After washing with PBS, OPCs were incubated with O1, an antibody that recognizes the myelin typical lipid galactosylceramide (1:10, kind gift of Guus Wolswijk), followed by incubation with appropriate FITC-conjugated antibodies (1:50) for 25 min. Primary and secondary antibodies were diluted in 4% BSA for the OPCs. Nuclei were counterstained with 1 µg/ml DAPI (Sigma). Slides were mounted in Dako mounting medium and analyzed with a conventional fluorescence microscope (Provis AX70, Olympus, New Hyde Park, NY or Leica DM2000 LED). MBP^+ and $O1^+$ cells were counted and $MBP^+/O1^+$ ratios were calculated. All analyses were conducted in a blinded manner. A representative image is shown in SI appendix Fig. S5.

Quantitative PCR

RNA was isolated from the brains using the RNeasy Lipid Tissue Mini Kit (Qiagen, Venlo, The Netherlands) according to manufacturer's instructions. Conversion of RNA to cDNA was performed using qScript™ cDNA SuperMix (Quanta Biosciences, Gaithersburg, USA). Quantitative PCR was performed utilizing a StepOnePlus Real-Time PCR detection system (Life technologies) and universal cycle conditions (20s at 95°C, 40 cycles of 3s at 95°C and 30s at 60°C). The PCR reaction consisted of fast SYBR green master mix (Life technologies), 10 µM forward and reverse primers (SI appendix Table S1; Eurogentec, Seraing, Belgium), RNase-free water and 12.5 ng template cDNA. Expression was normalized using the two most stable reference genes and converted to fold-change as compared to healthy mice using the comparative Ct method.

Transmission electron microscopy

Sample preparation for transmission electron microscopy (TEM) was performed as previously described with minor modifications (11). Mice were transcardially perfused with Ringer's solution, followed by 2% glutaraldehyde in 0.05 M cacodylate buffer (pH 7.3) at 4°C. A coronal block of the CC (1 mm thick) within the anterioposterior coordinates from -0.3 to -1.5 mm was cut in midsagittal plane. Tissue blocks were post-fixed in 2% osmium tetroxide (Aurion, Wageningen, the Netherlands), dehydrated through graded concentrations of acetone and embedded in araldite epoxy resin (Aurion). To delineate the region of interest, semithin sections of 0.5 µm were cut using a Leica EM UC6 ultramicrotome (Leica, Groot-Bijgaarden, Belgium) and stained with 0.1% thionin and methylene blue solution for light microscopic selection. Ultrathin sections of 0.06 µm were mounted on 0.7% formvar-coated 50-µm mesh copper grids (Aurion) and automatically contrasted using a Leica EM AC20 (Leica) with 0.5% uranyl-acetate followed by a stabilized solution of lead citrate (both from Laurylab, Saint Fons, France). TEM analysis was performed with a Philips EM208 transmission electron microscope (Philips, Eindhoven, The Netherlands) equipped with a Morada Soft Imaging System camera (Olympus SIS, Münster, Germany). The G-ratio was calculated as axon diameter/fiber diameter in five representative images per animal in which 50 fibers per image were analyzed using Image J software. All analyses were conducted in a blinded manner.

Statistical analysis

Statistical analysis was performed using GraphPad Prism 7.04 software (GraphPad software Inc., CA, USA). Differences between group means were determined using a one-sample t-test, one-way or two-way ANOVA with Tukey's or Dunnett's multiple comparison test, respectively. All data depicted as mean ±SEM, *=$p<0.05$, **=$p<0.01$, ***=$p<0.001$ and ****=$p<0.0001$. For all experiments biological replicates were conducted.

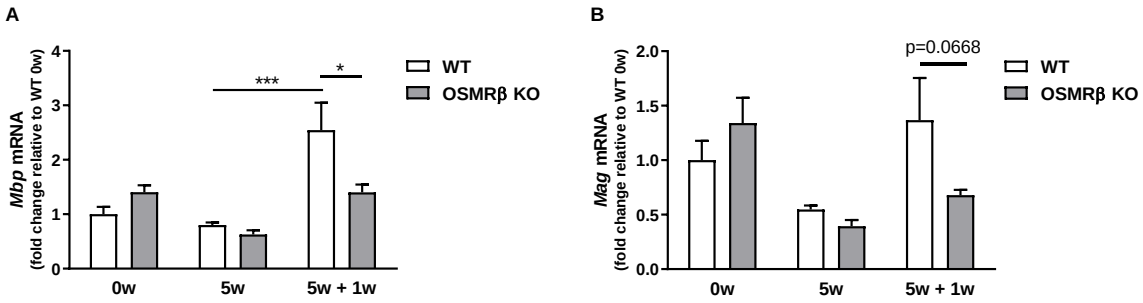

Fig. S1 *Mbp* and *Mag* expression in WT and OSMRβ KO mice on an acute cuprizone diet. mRNA expression of *Mbp* **(A)** and *Mag* **(B)** was measured in the CC of WT and OSMRβ KO mice receiving a normal diet (n= 5 per group), a cuprizone diet for 5 weeks and a cuprizone diet for 5 weeks followed by 1 week normal diet. Data are depicted as mean ± SEM. Two-way ANOVA with multiple comparison and Tukey's post hoc test. WT, wild type; KO, knock-out.

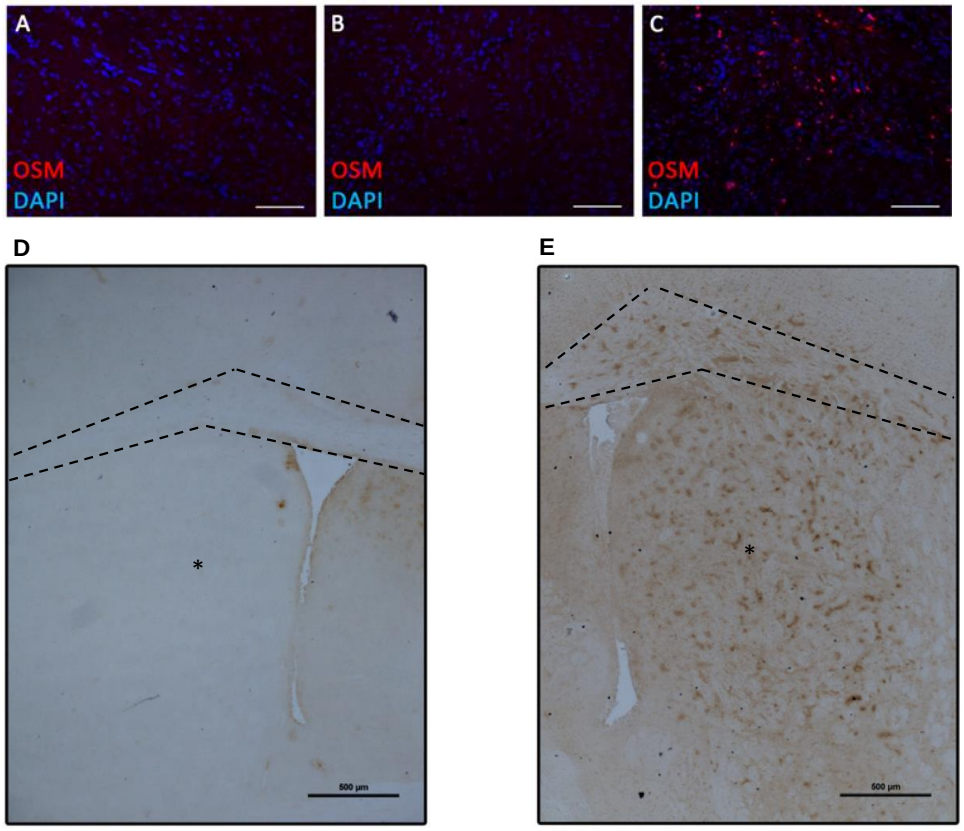

Fig. S2 LV-mediated expression of OSM in the brain of cuprizone-challenged mice. After 11 weeks of cuprizone diet, mice were injected with LV-OSM or LV-eGFP in the right striatum. Immunoreactivity for OSM in the LV-eGFP transduced hemisphere **(A)**, the contralateral hemisphere of LV-OSM transduced brain **(B)** and LV-OSM transduced hemisphere **(C)** 3 weeks after LV injection. OSM expression in the contralateral hemisphere **(D)** and transduced hemisphere **(E)** 6 weeks after LV-OSM transduction. The pictures show both CC (between dashed lines) and striatum (*) **(D,E)**. Scale bars represent 100 µm **(A-C)** or 500 µm **(D,E)**.

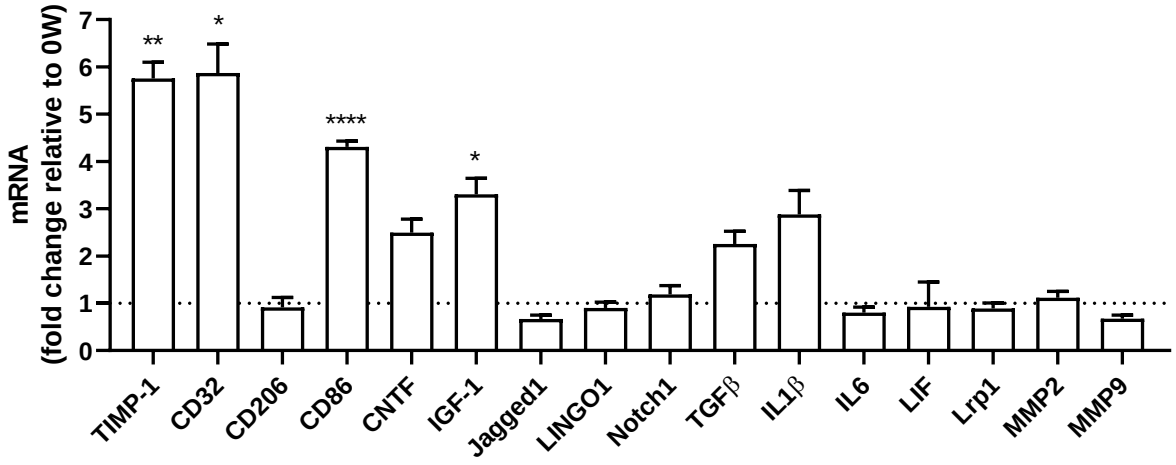

Fig. S3 mRNA expression during acute demyelination. mRNA expression of M1/M2/phagocytosis markers (*Cd32, Cd86, Cd206, Lrp1*) trophic factors (*Cntf, Lif, Igf-1, Timp-1*), inhibitory molecules (*Notch1, Jagged1, Lingo-1*), pro- and anti-inflammatory cytokines (*Il-1β, IL-6, Tgf-β*) and matrix metalloproteinases (*Mmp2, Mmp9*) measured using qPCR (n=5 per group). Brain tissue of WT mice was used after acute demyelination (5 weeks cuprizone diet) Expression is converted to fold change as compared to healthy animals. Data are depicted as mean ±SEM, *p<0.05, **p<0.01, and ****p<0.0001. Two-way ANOVA with multiple comparison Sidak's post hoc test.

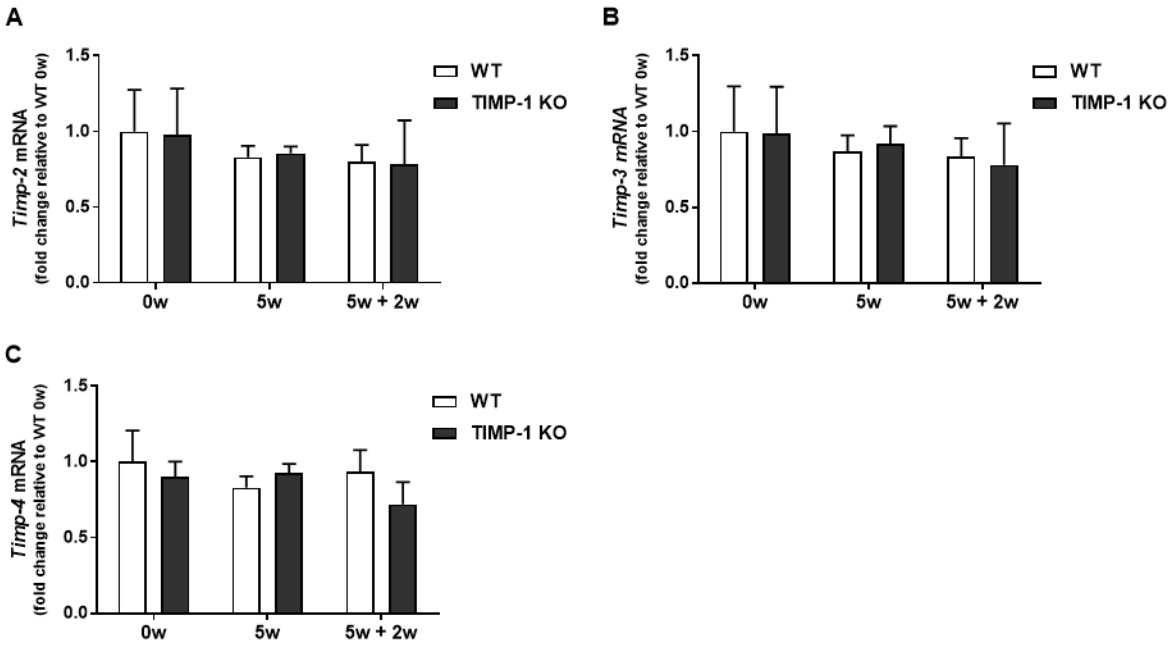

Fig. S4 Absence of compensatory expression by the genes encoding TIMP-2, TIMP-3 and TIMP-4. mRNA expression of (a) *Timp-2*, (b) *Timp-3* and (c) *Timp-4* was measured in the CC of WT and TIMP-1 KO mice receiving a normal diet (n= 5 or 6 per group), a cuprizone diet for 5 weeks (n=5 per group) and a cuprizone diet for 5 weeks followed by 2 weeks normal diet (n=5 or 6 per group). Data are depicted as mean ± SEM. Two-way ANOVA with multiple comparison and Tukey's post hoc test. WT, wild type; KO, knock-out.

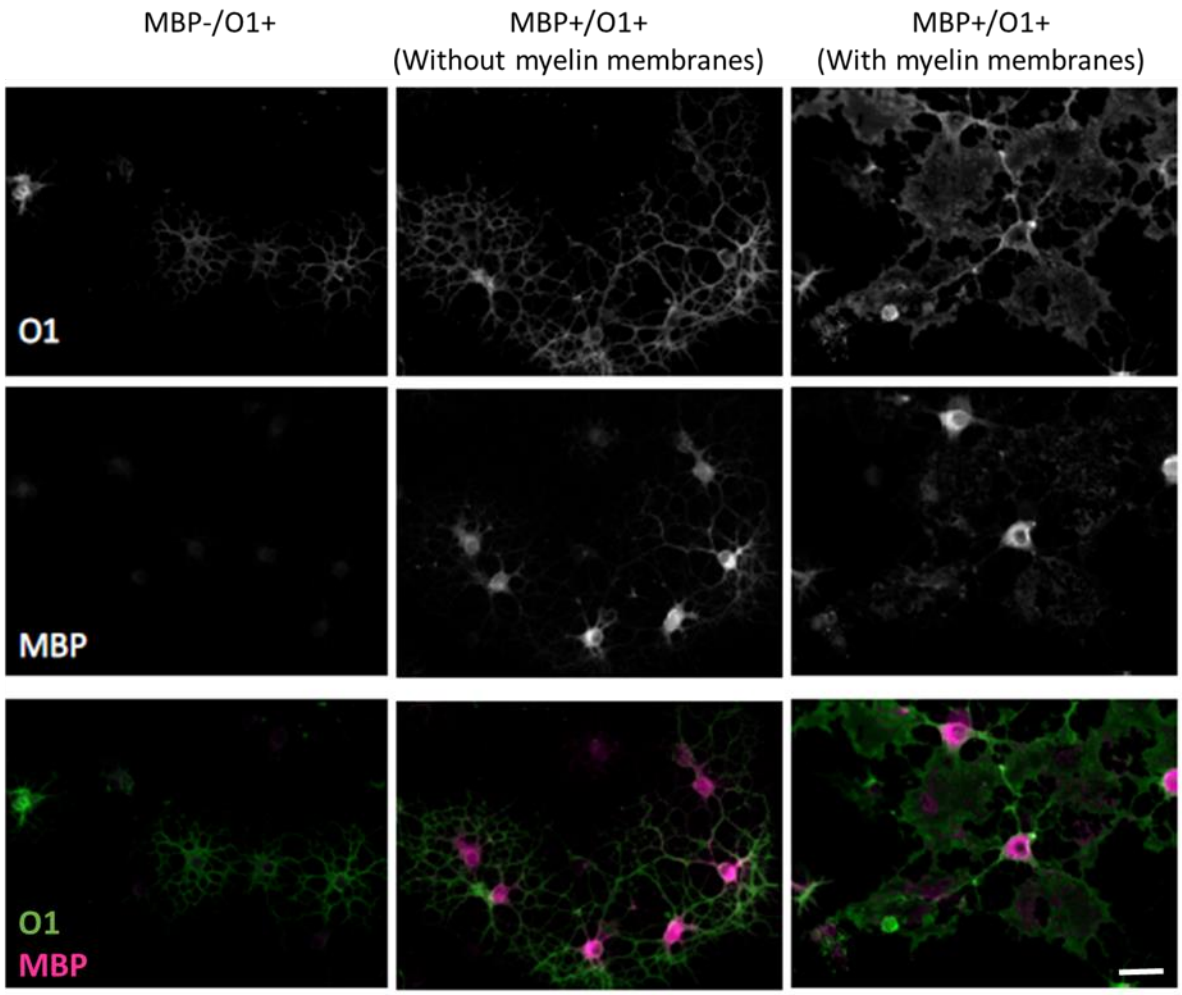

Fig. S5 Representative images for MBP+ oligodendrocyte (purple) /01+ cell (green) quantification. Scale bar represents 25µm.

Table S1. Mouse primer sequences used for qPCR

Gene	Forward primer (5′->3′)	Revers primer (5′->3′)
Hprt	CTCATGGACTGATTATGGACAGGAC	GCAGGTCAGCAAAGAACTTATAGCC
Tbp	ATGGTGTGCACAGGAGCCAAG	TCATAGCTACTGAACTGCTG
Rpl13a	GGATCCCTCCACCCTATGACA	CTGGTACTTCCACCCGACCTC
Cd206	ACCAAAGCTGACCAAAGGAAGA	AAAGGTGGGCTCTTGAGGTATG
Cd32	AGCAGGTTCCAGACAATCCTC	CCCAATGCCAAGGGAGACTAA
Cd63	AGAGACCAGGTGAAGTCAGAG	AGTCTGTGTAGTTAGAAGCTCCA
Cd86	ACTGTCAGTGATCGCCAACT	CACACACCATCCGGGAATGA
Cntf	AGAGAGTGCATTTCACCCCG	TCTGTTCCAGAAGCGCCATT
Igf-1	TACTTCAACAAGCCCACAGGC	ATAGAGCGGGCTGCTTTTGT
Il-1β	ACCCTGCAGCTGGAGAGTGT	TTGACTTCTATCTTGTTGAAGACAAACC
Il-6	TGTCTATACCACTTCACAAGTCGGAG	GCACAACTCTTTTCTCATTTCCAC
Jagged1	GCAGTCCCCATCCTTGTTAC	GGGAAGACTGGCACTCATTG
Lif	AAAAGCTATGTGCGCCTAACA	GTATGCGACCATCCGATACAG
Lingo-1	ACCTTCGCCTTCATCTCCAA	CAGGCAGAATAGGACAACGC
Lpar1	GAGGAATCGGGACACCATGAT	ACATCCAGCAATAACAAGACCAATC
Lrp1	TCAGACGAGCCTCCAGACTGT	ACAGATGAAGGCAGGGTTGGT
Mag	GCGTCATGTATGCACCTTGGA	GTGGAACACAGGATGGAGACTG
Mbp	GGCTGTGCCACATGTACAAGGACT	TGGGAT GGAGGTGGTGTTCGAGG
Mmp2	CGAGGACTATGACCGGGATA	GTGCAGCTCTCATACTTGTTG
Mmp9	GACATAGACGGCATCCAGTATC	GTGGGAGGTATAGTGGGACA
Notch1	CGCAAGAGGCTTGAGATGC	ATTGGAGTCCTGGCATCGTT
Osmrβ	TCACAACTCCAGATGCACGC	ACTTCTCCTTCACCCACTGAC
Tgf-β	GGGCTACCATGCCAACTTCTG	GAGGGCAAGGACCTTGCTGTA
Timp-1	GGACCTGGTCATAAGGGCTA	TACCGGATATCTGCGGCATT
Timp-2	CCAAGTGGGTTCACGCTAGT	GAAGGGGTATGGCAGGGAAC
Timp-3	CACGGAAGCCTCTGAAAGTC	TCCCACCTCTCCACAAAGTT
Timp-4	ACCTCCGGAAGGAGTACGTT	TTATCTGGCAGCAACACAGC

References

1. M. Tanaka, Y. Hirabayashi, T. Sekiguchi, T. Inoue, M. Katsuki*, et al.*, Targeted disruption of oncostatin M receptor results in altered hematopoiesis. *Blood*. **102** 3154-62 (2003).
2. K. Nakamura, H. Nonaka, H. Saito, M. Tanaka, A. Miyajima, Hepatocyte proliferation and tissue remodeling is impaired after liver injury in oncostatin M receptor knockout mice. *Hepatology*. **39** 635-44 (2004).
3. H. Lassmann, M. Bradl, Multiple sclerosis: experimental models and reality. *Acta Neuropathol*. **133** 223-44 (2017).
4. V. Baekelandt, A. Claeys, K. Eggermont, E. Lauwers, B. De Strooper*, et al.*, Characterization of lentiviral vector-mediated gene transfer in adult mouse brain. *Hum Gene Ther*. **13** 841-53 (2002).
5. H. Slaets, J.J. Hendriks, C. Van den Haute, F. Coun, V. Baekelandt*, et al.*, CNS-targeted LIF expression improves therapeutic efficacy and limits autoimmune-mediated demyelination in a model of multiple sclerosis. *Molecular therapy : the journal of the American Society of Gene Therapy*. **18** 684-91 (2010).
6. K. Janssens, A. Maheshwari, C. Van den Haute, V. Baekelandt, P. Stinissen*, et al.*, Oncostatin M protects against demyelination by inducing a protective microglial phenotype. *Glia*. **63** 1729-37 (2015).
7. A. Maheshwari, K. Janssens, J. Bogie, C. Van Den Haute, T. Struys*, et al.*, Local overexpression of interleukin-11 in the central nervous system limits demyelination and enhances remyelination. *Mediators of inflammation*. 2013;:685317 doi: 10.1155/2013/ (2013).
8. D. Lentferink, J. Jongsma, I. Werkman, W. Baron, Grey matter OPCs are less mature and less sensitive to IFNγ than white matter OPCs: consequences for remyelination. *Sci Rep*. **8** 2113- (2018).
9. J.L. Mason, A. Toews, J.D. Hostettler, P. Morell, K. Suzuki*, et al.*, Oligodendrocytes and progenitors become progressively depleted within chronically demyelinated lesions. *Am J Pathol*. **164** 1673-82 (2004).
10. M. Kipp, T. Clarner, J. Dang, S. Copray, C. Beyer, The cuprizone animal model: new insights into an old story. *Acta Neuropathol*. **118** 723-36 (2009).
11. T. Struys, A. Ketkar-Atre, P. Gervois, C. Leten, P. Hilkens*, et al.*, Magnetic resonance imaging of human dental pulp stem cells in vitro and in vivo. *Cell Transplant*. **22** 1813-29 (2013).